THE INTERACTION OF THE FLOTATION REAGENT, N-OCTANOHYDROXAMATE, WITH SULFIDE MINERALS.

Gretel Parker[a*], Alan Buckley[b], Ronald Woods[a] and Greg Hope[a].

a. Queensland Micro- and Nanotechnology Centre, Griffith University, Nathan, QLD, 4111, Australia.

b. The University of New South Wales, Sydney, NSW, 2052, Australia.

Abstract

We have utilised electrochemistry, vibrational spectroscopy and X-ray photoelectron spectroscopy in order to investigate the interaction of n-octanohydroxamate with sulfide minerals, including chalcocite, pyrite, chalcopyrite, covellite and bornite. In the presence of hydroxamate, each of these techniques showed that on chalcocite, bornite and chalcopyrite a multilayer of cupric hydroxamate was formed, and that this multilayer rendered the mineral hydrophobic. Ferric n-octanohydroxamate was also observed on the ternary sulfides. These results have implications in the use of hydroxamates for the flotation of mixed sulfide-oxide and transitional ores.

Keywords: sulfide minerals, electrochemistry, Raman spectroscopy, X-ray photoelectron spectroscopy, hydroxamate.

Background

Declining orebody quality means that low-grade and complex ores are increasingly being considered for recovery of their valuable metals. Such ores, including low-grade oxide ores, transitional ores and tarnished former tailings or waste rock will need further beneficiation to make them amenable to smelting or hydrometallurgical processing. Flotation with controlled potential sulfidisation is one approach that is used, but chemical control can be difficult and costly. Hydroxamates were proposed by Pöpperle in 1940 as collectors for both sulfide and oxide ores (Pöpperle, 1940), but subsequent studies have yielded equivocal results for the hydroxamate flotation of sulfide minerals. Another approach would be to use mixed oxide-sulfide collector systems (Lee et al., 2009). It is, therefore, important

* Corresponding author. Tel: +61 7 3735 3656; E-mail address: G.Heber@griffith.edu.au.

to characterise the interaction of sulfide mineral surfaces with hydroxamate collectors, such as n-octanohydroxamate.

The interaction of n-octanohydroxamate with some sulfide minerals has been reported. Notably, pyrite was floated along with chrysocolla, the target mineral, with hydroxamate collector (Fuerstenau et al., 1967), although another study showed minimal recovery of pyrite with hydroxamate between pH 5 and 10.5 (Ackerman et al., 1999). Electrochemical studies (Hanson and Fuerstenau, 1987, 1991) have demonstrated the feasibility for potassium n-octanohydroxamate to be a collector for chalcocite and oxidised copper ores, but Fuerstenau reported that the copper sulfide minerals chalcopyrite and covellite were not rendered hydrophobic by hydroxamate (Fuerstenau et al., 2000). Elsewhere 'oxidised' chalcopyrite has been reported to float with hydroxamate (Das and Pradip, 1987), with moderate recoveries reported for chalcopyrite, covellite and bornite compared to high recovery (94%) of chalcocite at pH 8.5 (Ackerman et al., 1999). Under the same conditions the recovery of malachite was only 60%, suggesting the collector concentration used was probably too low. In order to elucidate possible reasons for these conflicting findings, there is a need to study the surface interactions between sulfide minerals and n-octanohydroxamate at concentrations comparable to those used in practice.

Experimental

Minerals and Reagents

Electrolyte and reagent solutions were made with Analytical Reagent (AR)-grade chemicals and doubly de-ionized (DDI) water. Potassium hydrogen n-octanohydroxamate was supplied by Axis House, Australia, a company which markets this compound within its AM2 flotation formulation. The potassium salt was recrystallised from methanol and dried in air. The n-octanohydroxamic acid was precipitated by treating a solution of the potassium salt dissolved in hot methanol with sulfuric acid, chilling and adding DDI water: the precipitate was filtered and washed with DDI water and dried in air. The sample was then recrystallized from ethyl acetate and dried in air before investigation. Copper n-octanohydroxamate was synthesized using a two-phase technique; copper acetate was dissolved in water and the hydroxamic acid was dissolved in diethyl ether. The hydroxamic acid phase was carefully added to the aqueous phase held in a test tube and the tube sealed. The solid copper salt formed at the interface between the aqueous and organic phases. The resultant solid was collected by filtration, washed with 0.1 M KOH to remove

residual hydroxamic acid, rinsed with DDI water and dried in air. Ferric n-octanohydroxamate was synthesized by dissolving ferric chloride in water and mixing with n-octanohydroxamic acid dissolved in ethanol: potassium carbonate was added to the ethanol/water mixture until a precipitate formed. The precipitate was recrystallized from ethanol:water (1:1).

The mineral specimens investigated were bornite from the Central African Copperbelt, chalcopyrite from the Messina Transvaal, pyrite from China and Spain and chalcocite and covellite from Butte, Montana. The minerals were conditioned with hydroxamate solutions after fracture or after abrading with 600 or 1200 grit SiC paper and rinsing/ultrasonicating with DDI water. Unless otherwise stated, specimens were treated with a freshly-prepared, nominally saturated aqueous solution (~0.02 M) of pure potassium hydrogen n-octanohydroxamate at its unadjusted pH (~9.5) in air at ambient temperature. This pH was selected as it is near the middle of the range used in practice for this collector with oxide copper ores (Hughes, 2007; Lee et al., 2009). The relatively high concentration was used on the basis that in practice, up to 1200 g/t of hydroxamate collector is utilized (Lee et al., 2009).

Raman Spectroscopy

Raman studies were conducted on a Renishaw System 100 or InVia Raman spectrometer. The System 100 and InVia spectrometers used 632.8 nm red excitation from a HeNe laser. The scattered light was detected with Peltier-cooled CCD detectors with spectral resolution ~ 2 cm^{-1}. In the case of the System 100, the laser and scattered radiation were focused through the spectrometer objective, an ultra long working distance x20 Olympus Plan Fl lens (NA=0.4), while on the InVia spectrometer the laser and scattered light were usually focused through a x50 Leica N Plan lens (NA=0.75). Raman spectra were calibrated using the 520 cm^{-1} silicon band. Spectral manipulations such as baseline adjustment, smoothing and normalisation were performed either with the Renishaw WiRE 3.2 software or with GRAMS32AI software (Galactic Industries, Salem, NH, USA).

Electrochemistry

Sulfide mineral electrodes were prepared for electrochemical experiments by attaching copper wire to the mineral specimens with silver-loaded epoxy, encasing the copper wire in Teflon shrink tubing and covering the join with epoxy resin. Potential control of the conventional three electrode cell (sulfide mineral working electrode, Ag/AgCl reference electrode and Pt counter electrode) was maintained with a Pine Wavenow USB potentiostat interfaced

with a PC running Pine Aftermath software V1.2.4361. All potentials are reported against the Ag/AgCl (3.0 M KCl) reference electrode.

X-ray Photoelectron Spectroscopy

X-ray photoelectron spectra were collected from a surface of single piece mineral specimens of area approximately 5 mm x 5 mm: there are numerous advantages to be gained by the characterisation of such surfaces in flotation-related research (Buckley, 2010), most importantly the facility of rinsing any weakly adsorbed collector from the surface, and the ability to determine by visual examination whether that surface had been rendered hydrophobic by interaction with the collector. Each fracture surface, or surface abraded until relatively smooth to the unaided eye, was rinsed with water after conditioning in collector solution and before characterisation by XPS at ambient temperature.

XPS data were obtained on an ESCALAB 250Xi spectrometer using monochromatised Al K_α X-rays focused to a spot size of 0.5 mm and an electron analyser pass energy of 20 eV for narrow range scans. Included in the binding energies employed for calibration were 83.96 eV for Au $4f_{7/2}$ of metallic gold and 932.6 eV for Cu $2p_{3/2}$ of Cu metal. The pressure in the analysis chamber was better than 5×10^{-9} mbar during spectral acquisition. In most cases, photoelectron spectra were obtained initially without the use of a flood gun, in which case the outermost strata of any adsorbed multilayer would be expected to experience some charge-shifting, and subsequently under the influence of flood gun electrons when the semi-conducting sulfide mineral substrate would remain largely unaffected, but adsorbed layers would be shifted to lower binding energy to an extent that would depend on the effectiveness of their electrical contact with the substrate. In those cases, binding energies were referenced to 285.0 eV for the hydrocarbon C 1*s* photoelectrons. Whenever the flood gun was used, the possibility of beam damage by the low energy electrons was monitored. However, in all cases, spectra were obtained as quickly as possible, at the expense of signal-to-noise, in order to minimise any damage arising from the secondary electrons associated with the X-ray photoemission.

Results

Electrochemical studies

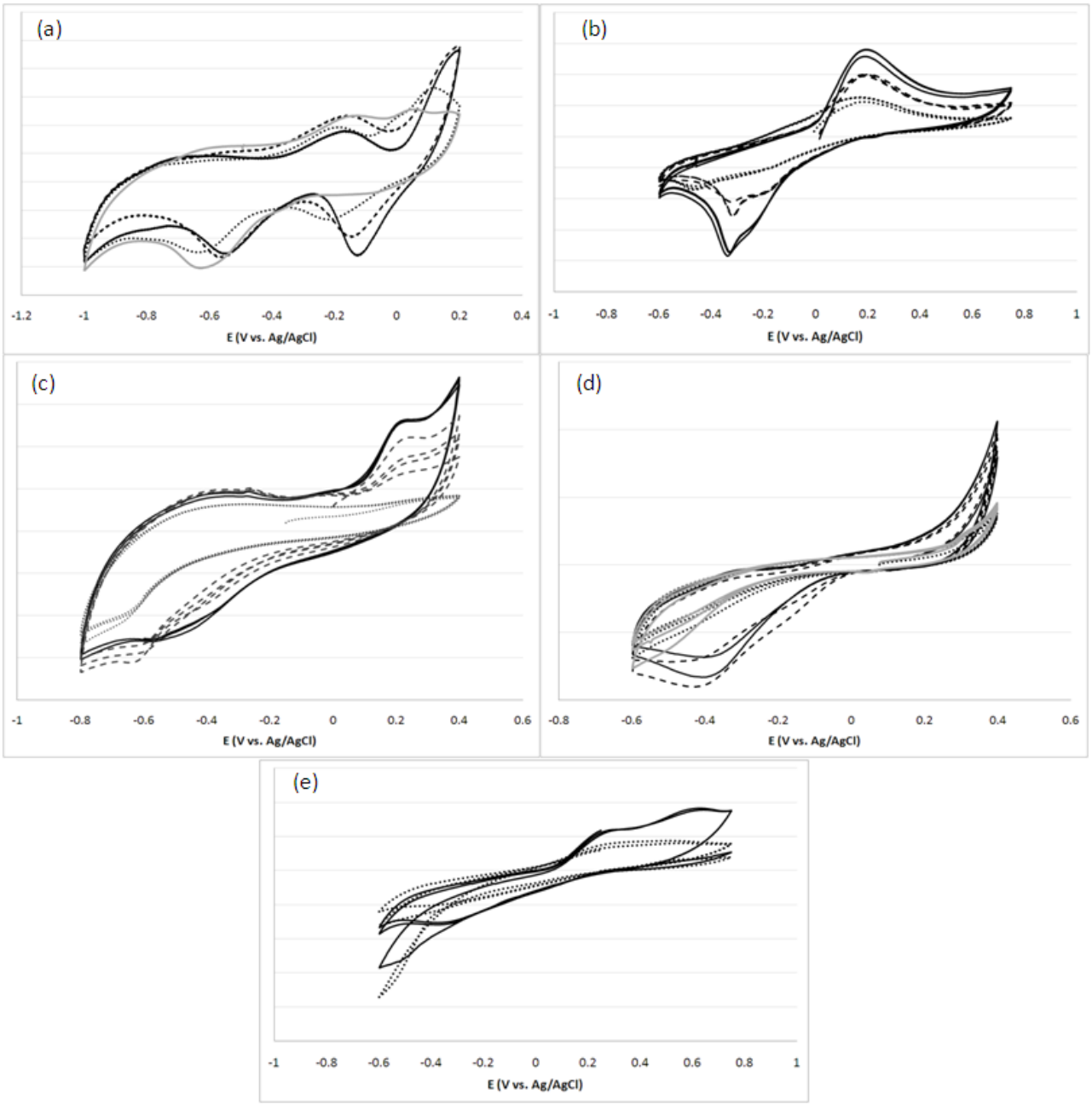

Fig. 1 Cyclic voltammograms from sulfide minerals (a: bornite; b: chalcocite; c: chalcopyrite; d: pyrite; e: covellite) in 0.05M sodium tetraborate with or without the addition of n-octanohydroxamic acid (solid black line: 0 mM; dashed line: 1 mM; dotted line: 5 mM; solid grey line: 10 mM n-octanohydroxamic acid) (sweep rate 25 mV/s).

We have reported the voltammetry from a bornite electrode in hydroxamate solutions (Fig. 1a) previously (Parker et al., 2011). As n-octanohydroxamate concentrations exceeded 1 mM the Cu(II) oxide reduction process at ~-0.1 V *vs.*

Ag/AgCl is reduced as cupric n-octanohydroxamate has been produced in the preceding forward-going scan. There are also some changes to the iron removal and re-insertion potentials to the sulfide lattice (Parker et al., 2011).

Cyclic voltammograms from a chalcocite electrode in tetraborate (Fig. 1b) were consistent with previously published voltammograms in the absence of the collector. Anodic current commenced flowing at approximately ~-0.1 V, with the anodic process resulting in the formation of intermediate non-stoichiometric copper sulfide phases (Hanson and Fuerstenau, 1987; Parker et al., 2003) and cupric hydroxide. This reaction is reversed in the negative-going scan. The addition of hydroxamate affects the redox behaviour of chalcocite by decreasing the peak anodic current and shifting the onset of anodic current to more negative values, which has been reported previously (Hanson and Fuerstenau, 1987). At sufficiently high concentrations the oxidation and reduction of the sulfide phases becomes inhibited, indicating multilayer formation of cupric n-octanohydroxamate.

The voltammogram from chalcopyrite (Fig. 1c) in the absence of hydroxamate shows a significant anodic process occurring at about ~0.2 V *vs.* Ag/AgCl, consistent with voltammetry reported elsewhere (Buckley and Woods, 1984; Gardner and Woods, 1979) and due to migration of iron from the sulfide lattice. The remaining iron-deficient copper sulfide lattice commences oxidation at higher potentials, forming cupric hydroxide and a metal-deficient sulfide phase. The preceding peaks are due to the oxidation of intermediate sulfides and oxy/hydroxide species on the surface. As expected, these intermediate species are not much affected by the addition of hydroxamate. However, both oxidation and reduction processes are significantly affected by hydroxamate if the concentration is sufficiently high. Notably, the iron migration from the sulfide lattice at ~0.2 V is affected and its corresponding insertion into the lattice at ~-0.5V is reduced but only after a few voltammetric cycles. This indicates that the underlying chalcopyrite can continue to react in the presence of the product hydroxamate and that multilayers are formed that remain insoluble under the conditions of the experiment. Results for bornite showed less suppression of the iron oxidation than was observed for chalcopyrite (Parker et al., 2011).

The voltammogram measured from pyrite in tetraborate in the absence of collector demonstrates features typical of the system. There is a very small step at ~-0.3 V *vs*. Ag/AgCl which is due to ferrous oxidation, and which has been reported to be absent on rotated electrodes in acidified systems (Lehmann et al., 2000). The reduction process at -0.4 V is due to reduction of both ferric oxide and, as it decreases with successively cycling, sulfur or oxygen (Abraitis et al., 2000). As the hydroxamate concentration is increased a small oxidation, and corresponding reduction process,

becomes evident at 0.2 V. The decreased oxidation charge observed in the first sweep from open-circuit potential at each concentration demonstrates that oxidation products form on the pyrite surface at open-circuit potential. The consistency of the oxidation current in subsequent sweeps indicates that the hydroxamate product is not significantly soluble and the changes in behaviour with concentration indicate a multilayer is formed.

Finally, voltammograms from covellite in hydroxamate solution are presented in Fig 1e. Anodic current commenced flowing just before 0 V, and this shifted slightly in the presence of hydroxamate, due the formation of cupric n-octanohydroxamate, so formed when the chalcocite produced on the previous negative-going scan is oxidised. The initial negative-going scan in the presence of hydroxamate shows different reduction behaviour than is observed in succeeding scans, indicating that a product formed on the initial positive-going scan in the presence of hydroxamate is reduced and then solubilised or passivated: this is quite different to the behaviour of hydroxamate with the other sulfide minerals investigated, indicating that hydroxamate may interact with an oxidised covellite surface in a different manner than it does with the other sulfides. After the initial scan, the voltammogram is similar to that observed from chalcocite in hydroxamate solution.

There is no evidence for an anodic prewave on the voltammograms from any of the sulfides investigated when hydoxamate is present that could be identified with underpotential deposition of a chemisorbed species. This contrasts with the interaction of thiol collectors with sulfide minerals which display voltametric chemisorption prewaves. It would appear that chemisorption of hydroxamate and bulk metal hydroxamate formation take place in the same potential range.

Raman spectra

Raman spectra of the relevant reference compounds are displayed in Figure 2. We have published the band assignments of the acid and potassium hydrogen n-octanohydroxamate salt, demonstrating that the hydroxamate moiety in these compounds adopts the keto Z conformation and also that in the potassium salt one potassium ion is shared between two hydroxamate moieties along with a proton (Hope et al., 2010a). This hydrogen bonding through the solid salt causes NH band shifting and splitting compared to the acid. The solution spectrum (not shown) of potassium n-octanohydroxamate dissolved in KOH resembles that for the solid n-octanohydroxamic acid, with the carbonyl stretch obscured by the OH bending modes of water.

The bands of the cupric compound have been assigned and, together with elemental analyses and ^{15}N isotope substitution studies, demonstrate that one n-octanohydroxamate moiety is found for each Cu, and that the hydroxamate assumes an enol tautomeric form in which bonding through the two hydroxamate O atoms (as well as interaction with the N atom) occurs (Hope et al., 2011): thus there is no carbonyl band at ~1600 cm^{-1} or NH bands at ~3200 cm^{-1} in the copper compound, whereas in the ferric compound in which hydroxamate is bound in the keto conformation, these features are observed.

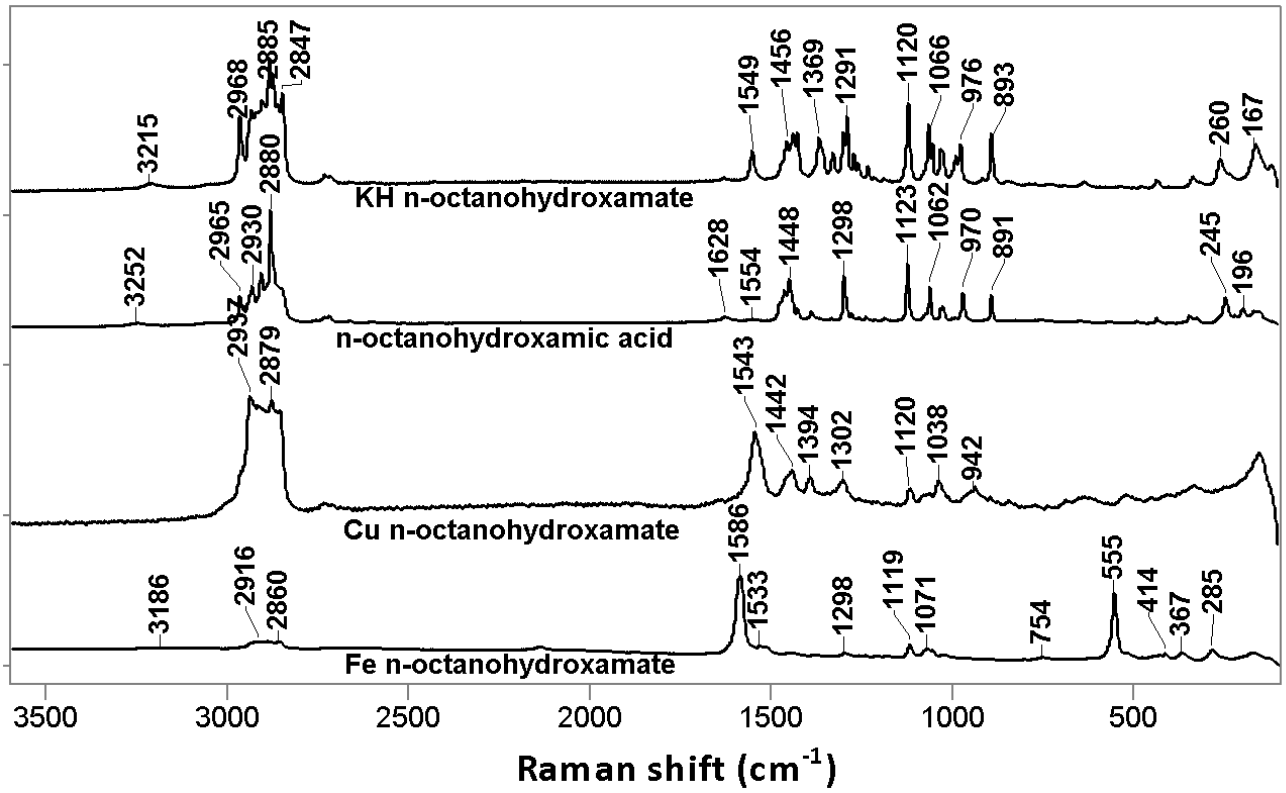

Fig. 2 Raman spectra of the potassium hydrogen-, cupric- and ferric n-octanohydroxamate compounds and n-octanohydroxamic acid.

Oxidation produced interference films on chalcocite, bornite (reported previously (Parker et al., 2011)) and pyrite. Such films were too thin to be detected by normal Raman spectroscopy, although bulk compounds formed at 'active' sites (grain edge boundaries) could be selectively sampled and are presented in Figures 3 to 6. No hydroxamate product was detectable via Raman spectroscopy on covellite. Cupric n-octanohydroxamate deposits were rarely evident on chalcocite and chalcopyrite and only at crystal intersections. A low intensity signal with a band at ~1550 cm^{-1}, indicative of cupric n-octanohydroxamate was evident on bornite surfaces conditioned for shorter periods (20 mins oxidation, 40 mins conditioning (Parker et al., 2011)). On chalcopyrite many discrete deposits of orange ferric

n-octanohydroxamate were evident over the entire exposed surface, compared to relatively few green cupric n-octanohydroxamate deposits at grain boundaries. Such behaviour was not evident on the conditioned pyrite specimen as the interference film appeared very uniform with very few discrete patches of ferric n-octanohydroxamate product located preferentially at crystal edge sites.

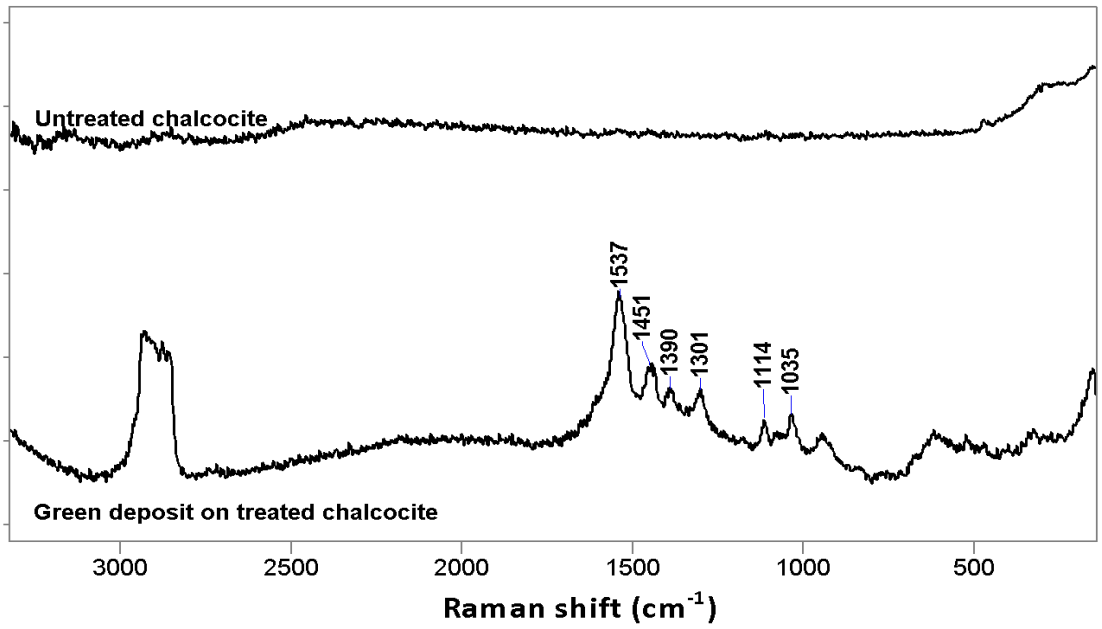

Fig. 3 Raman spectra from untreated chalcocite and chalcocite treated with 5 mM n-octanohydroxamic acid in 0.05 M sodium tetraborate for 5 days.

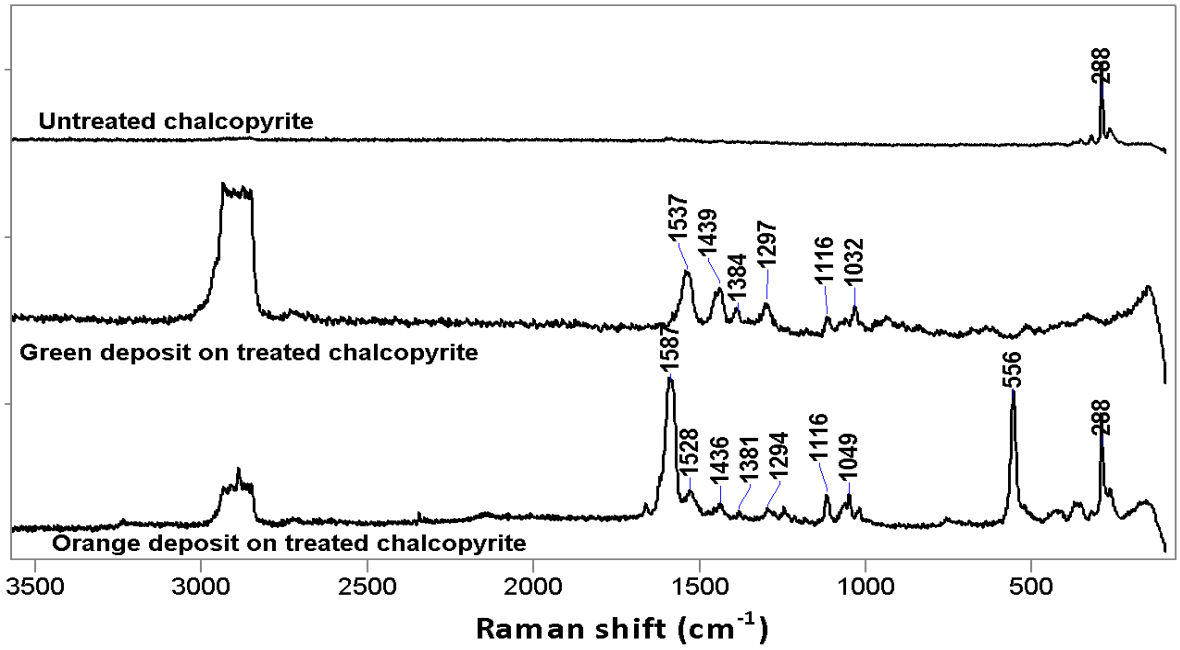

Fig. 4 Raman spectra from untreated chalcopyrite and chalcopyrite treated with 5 mM n-octanohydroxamic acid in 0.05 M sodium tetraborate for 5 days.

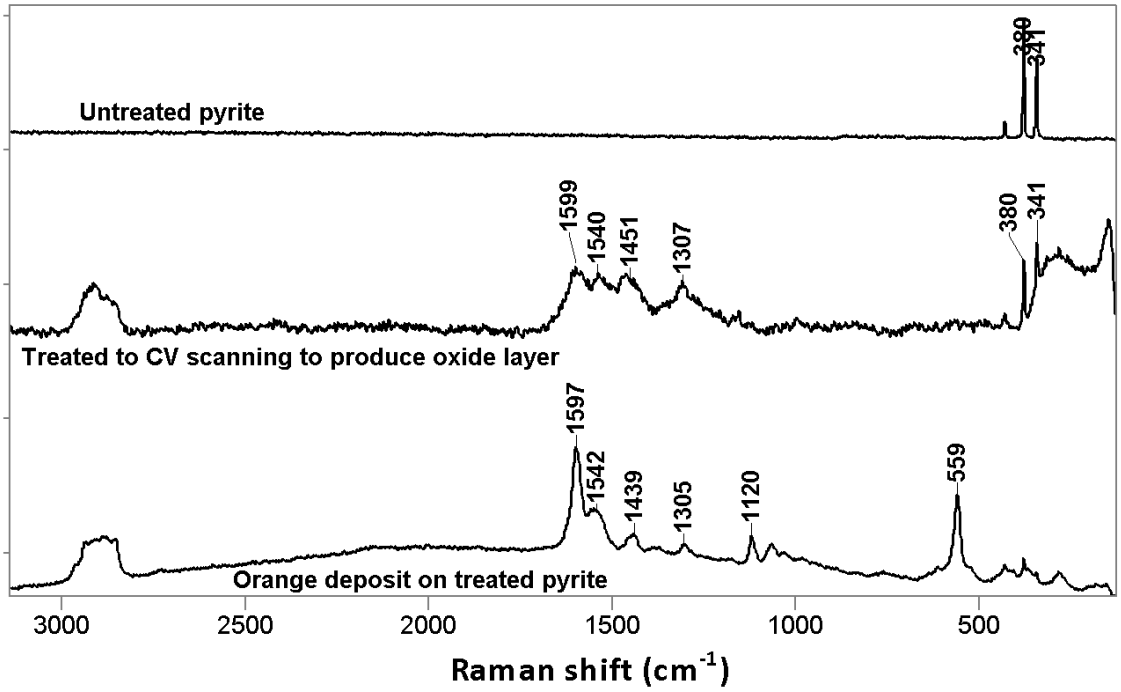

Fig. 5 Raman spectra from a pyrite specimen that is untreated, after CV scanning in hydroxamate to produce an oxide layer, and after grinding and exposing to air for 20 min then treating with saturated n-octanohydroxamate solution (pH unadjusted) for 40 min.

SERS study of n-octanohydroxamate interaction with pyrite

In situ SERS studies of a gold decorated pyrite electrode are displayed in Figure 6. This figure demonstrates that hydroxamate is adsorbed on the pyrite surface at negative potentials, but that the resonant carbonyl band is red-shifted at lower potentials, consistent with our ferrous/ferric hydroxamate studies (Parker et al., 2011) , and not consistent with hydroxamate sorbed on Au. Given the conditions of preparation of the electrode for the study, it is expected that the hydroxamate reacted with the ferric oxide before application of the potential: clearly the hydroxamate remains largely insoluble even under reducing conditions.

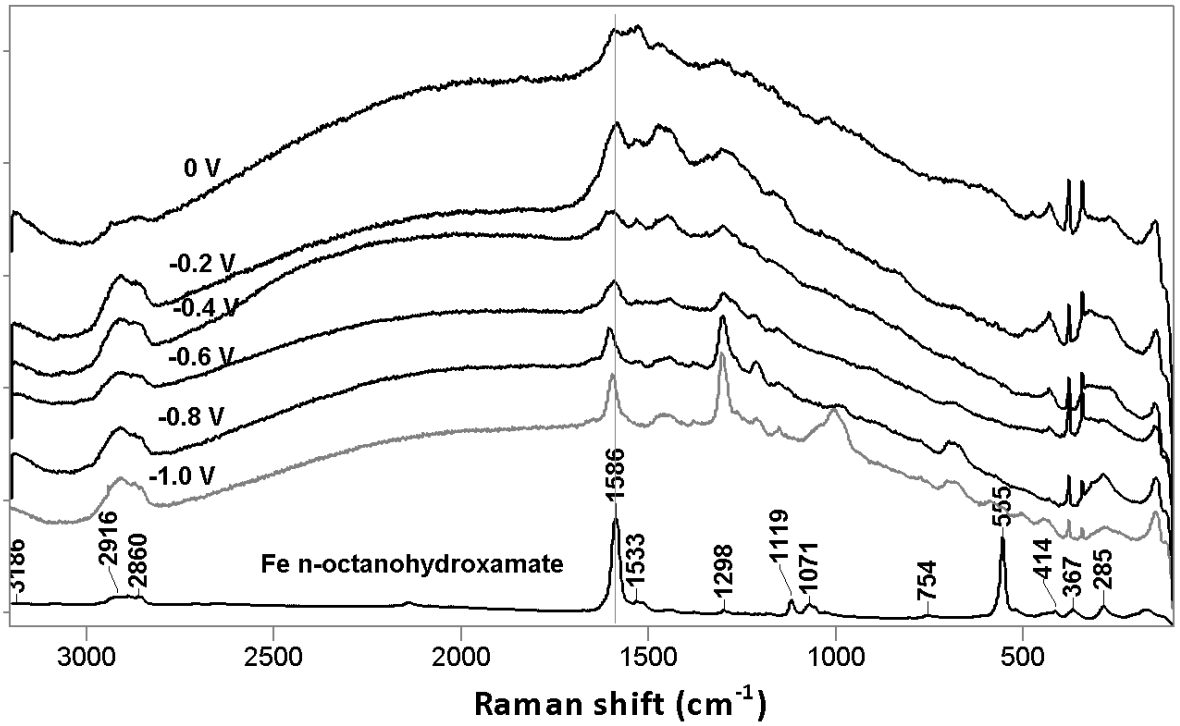

Fig. 6 Raman spectra from a gold-decorated pyrite surface in 1mM solution of potassium n-octanohydroxamate dissolved in 0.01 M potassium hydroxide at various applied potentials.

X-ray photoelectron spectroscopy

Chalcocite

Chalcocite surfaces that had been freshly abraded in air were conditioned in hydroxamate solution for periods of relevance to flotation (1-10 min) as well as for an extended period (2 h). Extended conditioning was included in the investigation to establish whether coverage reached a plateau under high collector concentration conditions, to establish whether the coverage was uniform or in patches, and to confirm the earlier conclusion that adsorbed multilayer Cu hydroxamate had a chemical structure similar to that of the bulk complex (Hope et al., 2010b; Hope et al., 2011). The conditioned surfaces were clearly hydrophobic.

Photoelectron spectra for a surface conditioned for 2 h were obtained initially without the use of low energy electrons from a flood gun. The surface N concentration was ~6.7 at%, lower than that for bulk Cu hydroxamate (~8 at%) but consistent with appreciable adsorption of collector. The principal component of the N 1*s* spectrum (Fig. 7) was at 400.0 eV, the binding energy expected for N that had been deprotonated but was interacting with a Cu atom in adsorbed Cu hydroxamate (N_d). Unresolved minor components at ~401 and ~402 eV accounted for the remaining

20% of the N 1*s* intensity. The component near 401 eV could be assigned to protonated N, possibly in co-adsorbed hydroxamic acid, and that near 402 eV would probably have been a charge-shifted component from N atoms in adsorbed hydroxamate that was in poor electrical contact with the substrate. The C 1*s* and O 1*s* spectra were also consistent with adsorbed hydroxamate and a similar degree of charge-shifting. There was no oxide component evident near 530 eV in the O 1*s* spectrum. As expected, the S 2*p* spectrum was less intense but otherwise similar to that for S in an unaltered Cu sulfide lattice, confirming that the S had remained in the substrate and had not been directly involved in the interaction with the collector. No potassium that might have been associated with any non-adsorbed collector that had not been rinsed from the surface was detected.

In the corresponding Cu 2*p* spectrum (Fig. 8), the Cu^{II} $2p_{3/2}$ principal peak and final state satellites had binding energies and intensities similar to those for bulk Cu hydroxamate. Also in that spectrum, the chalcocite substrate $2p_{3/2}$ peak remained evident, accounting for 20% of the total $2p_{3/2}$ intensity. The retention of the substrate peak in the relatively surface-sensitive Cu 2*p* spectrum indicated that the adsorbed hydroxamate coverage was limited either to no more than ~3 molecular layers if uniform, or to somewhat thicker layers if in patches. Fitting of the much less surface-sensitive Cu 3*p* spectrum revealed that the substrate doublet component accounted for 60% of the total Cu 3*p* intensity. These observations implied a substantially uniform coverage, as if the Cu hydroxamate were in thick patches, the substrate Cu^{I} detected would predominantly be that located between those patches, in which case the Cu^{II}:Cu^{I} intensity ratio should have been similar in both the Cu 2*p* and 3*p* spectra.

A largely uniform coverage was consistent with the observed small proportion of the adsorbed hydroxamate becoming charged as a result of photoemission. It was also consistent with the behaviour observed when spectra were determined under the influence of a low energy electron beam from a flood gun. With the flood gun on, the C 1*s*, O 1*s* and N 1*s* spectra all split into three partially-resolved components of comparable intensity, one shifted to lower binding energy by the full 4 eV electron energy, one shifted by about 2.5 eV, and one shifted by less than 1 eV. The component shifted by 4 eV would have been from N atoms in the layer furthest from, and hence in poorest electrical contact with, the substrate. The Cu 2*p* spectrum was more complex because the shifted principal Cu^{II} components became superimposed on the unaffected Cu^{I} substrate peak, but no Cu^{II} 2*p* intensity appeared to be shifted by less than 1 eV; all of it appeared to be shifted by either ~2.5 or 4 eV. These observations, together with the concentration ratio Cu^{II}:N_d being less than 1.0, were consistent with a monolayer of hydroxamate chemisorbed

to Cu atoms in the surface of the substrate, and 2-3 layers of Cu hydroxamate on top of the chemisorbed layer. The Cu^{I} to which the hydroxamate was chemisorbed could have reacted with oxygen and become hydroxylated prior to conditioning, and the OH^{-} subsequently exchanged by hydroxamate. In the absence of a chemisorbed layer, Cu^{II}:N_d should be $\geq$1, as while it might be possible for some Cu^{II} hydroxide that had been formed during air exposure to have remained at the surface after conditioning, the only deprotonated N with 1*s* binding energy 400.0 eV should have been Cu(hydroxamate) or chemisorbed hydroxamate. It had been deduced from XPS data for hydroxamate adsorbed to the native oxide on Cu metal that the N electronic environment in the chemisorbed collector was similar to that in multilayer Cu hydroxamate (Parker et al., 2011). This implies that the chemisorbed hydroxamate was initially oriented parallel with the surface, facilitating interaction of its N with a surface Cu atom. Any N in co-adsorbed hydroxamic acid would have had a 1*s* binding energy of ~401 eV. Even if $Cu(hydroxamate)_2$ did exist, and there is no evidence that it does under conditions of relevance to flotation, then that N too would be expected to have a 1*s* binding energy significantly greater than 400.0 eV. With a chemisorbed layer covered by only 2 molecular layers of Cu hydroxamate, Cu^{II}:N_d could be as low as 0.67:1. For chalcocite conditioned for 2 h, the ratio was 0.72, in line with 2-3 layers of adsorbed Cu hydroxamate.

The collector coverage on chalcocite surfaces conditioned for periods of 1-10 min was lower than for the 2 h treatment, nevertheless the spectra could be rationalised by an adsorbate structure similar to that described above. For the lowest coverage observed, the surface N concentration was ~7 at%, but the Cu^{II} concentration estimated from the Cu 2*p* spectrum was less than 2 at%, implying that most of the adsorbed hydroxamate was in a monolayer chemisorbed to Cu^{I} in the mineral surface. The Cu^{II} principal peak was at the same binding energy as that for multilayer and bulk Cu hydroxamate. Almost 80% of the N 1*s* intensity was at a binding energy of 400 eV, and Cu^{II}:N_d was 0.33. The component at ~401.3 eV accounted for 12% of the N 1*s* intensity, but unexpectedly, the remaining ~10% was at a binding energy greater than 402 eV, suggesting that a small proportion of the adsorbate, most probably co-adsorbed hydroxamic acid, was in poor electrical contact with the underlying chemisorbed layer. Again there was no oxide component near 530 eV in the O 1*s* spectrum, and no potassium at the surface.

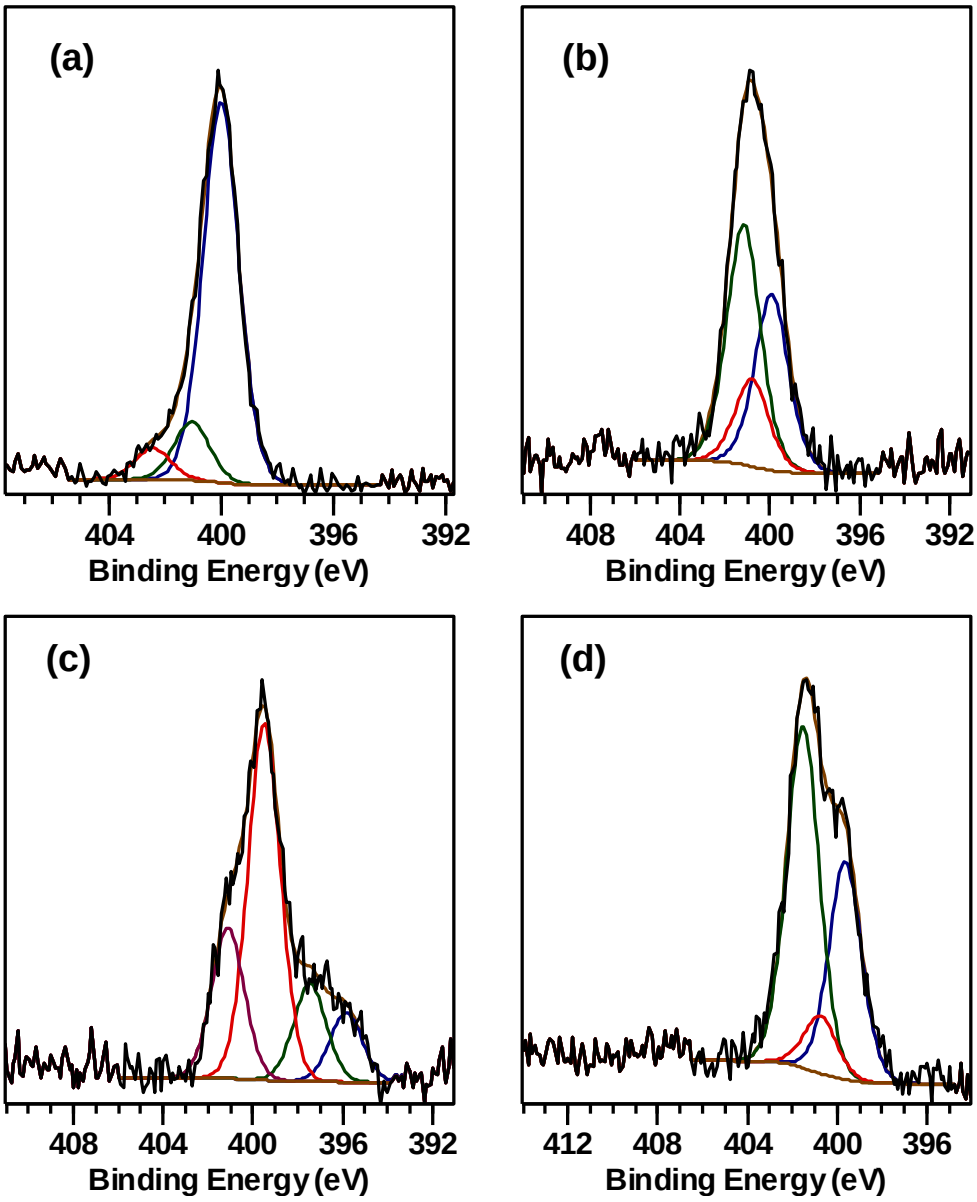

Fig. 7 N 1*s* spectrum from: (a) chalcocite conditioned in hydroxamate solution for 2 h; (b) chalcopyrite conditioned for 1 min; (c) chalcopyrite conditioned for 10 min under the influence of a 4 eV electron beam; (d) minimally oxidized bornite conditioned for 1 min.

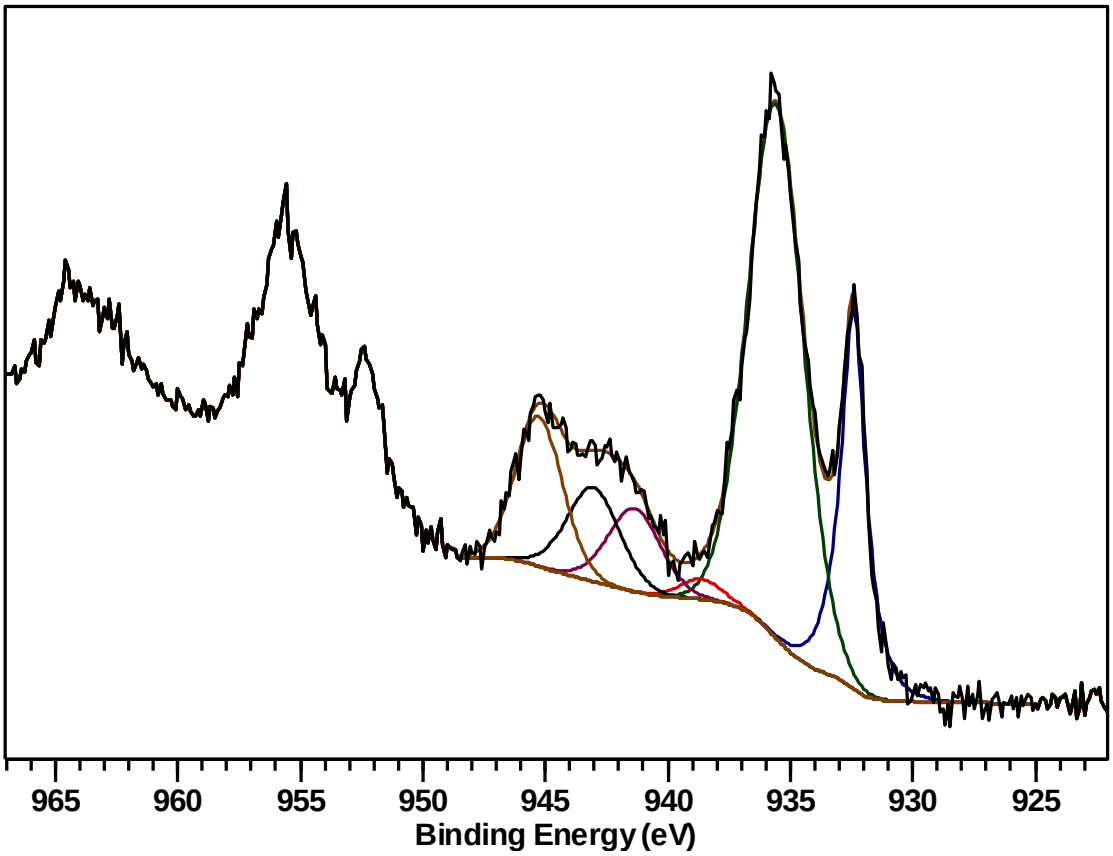

Fig. 8 Cu 2*p* spectrum from chalcocite conditioned in hydroxamate solution for 2 h.

Covellite

Covellite surfaces parallel to the {001} planes that had been abraded in air and subsequently rinsed with water without any conditioning in hydroxamate were hydrophilic. The O 1*s* intensity was quite low, with no oxide component near 530 eV. There was no energy loss peak near 946 eV in the Cu 2*p* spectrum that would have signified the formation of Cu^{I} oxide and no evidence for significant Cu^{II} formation.

Abraded surfaces of covellite conditioned in hydroxamate solution for 10-20 min showed no indication of being hydrophobic, regardless of whether they had been given prior exposure to air for up to 60 min. The Cu 2*p*, Cu 3*p*, Cu LMM, S 2*p*, O 1*s* and C 1*s* spectra from a conditioned surface were not noticeably different from those for an abraded surface rinsed with water. The O 1*s* intensity remained low after conditioning, and the N 1*s* intensity was also low. These observations indicated that there had been very little adsorption of hydroxamate, and certainly negligible adsorption of cupric hydroxamate. Since 85% of the N 1s intensity was at ~400.0 eV, if the N had been in an hydroxamate species, the adsorbate would have been consistent with hydroxamate chemisorbed to Cu atoms at the surface, but inconsistent with adsorbed hydroxamic acid. The Cu atoms to which the hydroxamate was

chemisorbed would most probably have been present as hydroxide on the covellite surface rather than Cu atoms in the outermost layer of the sulfide lattice. However, beyond the formation of a Cu/O monolayer at the surface of covellite, it is not expected that Cu would migrate readily from the sulfide lattice to enable the formation of multilayer cupric hydroxamate. Whereas Cu is able to migrate from chalcocite to form a series of stable Cu sulfide phases of lower Cu content such as digenite, $Cu_{1.8}S$, there is no stable Cu sulfide phase with Cu content lower than CuS apart from CuS_2, which is not believed to be formed at atmospheric pressure (Evans Jr., 1981).

The observations suggest that the chemisorbed layer alone is unlikely to render a macroscopic surface of covellite strongly hydrophobic. It appears that Cu atoms must migrate from the underlying sulfide lattice to allow the formation of cupric hydroxamate for hydrophobicity to be imparted to such a surface.

Pyrite

Low concentrations of Fe sulfate have been observed at pyrite fracture surfaces exposed for several minutes to air under ambient conditions or to alkaline aqueous solutions, with the formation of Fe^{III} hydroxy-oxide species evident after longer exposure (Buckley and Woods, 1987). Photoelectron spectra from fracture surfaces of the pyrite studied in the present investigation after their exposure to air for 10 min were in general agreement with the earlier findings. In addition to the principal S 2*p* doublet at a $2p_{3/2}$ binding energy of 162.4 eV, there were only low intensity doublets at ~165 and ~168 eV, the former (accounting for no more than 6% of the total 2*p* intensity) attributable to an Fe-deficient sulfide surface layer and the latter (3%) to sulfate. The Fe-deficient sulfide indicated some loss of Fe from the lattice to form an Fe oxide species as well as the sulfate. The O 1*s* component at ~530 eV that would have arisen from Fe oxide was much less intense than the broad principal component at ~531.3 eV that could be attributed to sulfate and hydroxide. A low intensity but obvious feature at 708.9 eV was evident in the Fe 2*p* spectrum, but that peak has been assigned to an Fe^{II}-S surface state (Schaufuß et al., 1998) rather than an Fe/O species. Any Fe^{II}/O or Fe^{III}/O species would be expected to have an Fe $2p_{3/2}$ component near 710 eV or 711 eV, respectively. However, there was no component that was even partly resolved from the 'tail' of the asymmetric lineshape of the pyrite $2p_{3/2}$ peak.

Conditioning of fracture surfaces of pyrite in hydroxamate solution for 10 min following brief exposure to air did not render those surfaces strongly hydrophobic. The N 1*s* spectrum obtained without the use of a flood gun was of low

intensity (2.5 at%), and comprised a principal component at 400.7 eV consistent with hydroxamate chemisorbed to Fe atoms, and a minor component at 398.5 eV consistent with deprotonated hydroxamate N atoms, or N that might have been in a degradation product resulting from X-ray (secondary electron) beam damage. The semi-resolved feature at ~708.7 eV adjacent to the principal $2p_{3/2}$ peak in the Fe 2*p* spectrum was unchanged, but there was a noticeably *lower* intensity in the 710–716 eV region that remained devoid of structure. This lower intensity indicated that there was a lower concentration of reacted Fe species at the mineral surface after conditioning in the collector solution than formed in air during the same period, an observation consistent with the presence of very little, if any, molecular Fe hydroxamate at the conditioned surface. The S 2*p* spectrum also indicated less reaction than in air insofar as the component from Fe-deficient sulfide was even lower, and no S/O species at all were discernible. The C 1*s* and O 1*s* spectra were consistent with a low concentration of adsorbed hydroxamate.

Pyrite surfaces immediately after abrasion and rinsing in air were appreciably altered compared with fracture surfaces exposed to air for a similar period. A higher concentration of oxidised Fe species was evident in the Fe 2*p* spectrum, and a slightly more intense Fe-deficient sulfide component was present in the S 2*p* spectrum. A C 1*s* component at 288.5 eV suggested the presence of surface layer carbonate, and the O 1*s* spectrum was consistent with the presence of some oxide as well as hydroxide, carbonate and sulfate. The concentration of sulfate or other S/O species evident in the S 2*p* spectrum was no greater than at the air-exposed fracture surface.

Abraded surfaces of pyrite conditioned in hydroxamate solution for 3 min were clearly hydrophobic, and the photoelectron spectra showed that significantly more hydroxamate was adsorbed at those abraded surfaces than at a fracture surface conditioned for 10 min. For the abraded surfaces, the concentration of N was almost 5%, and there was a sizeable Fe^{III} component that would have accounted for up to 25% of the Fe $2p_{3/2}$ peak. The N 1*s* spectrum obtained without the use of a flood gun was centred at 401.2 eV, but it was relatively broad and asymmetric, and a minor (15%) component near 399.3 eV, possibly from beam-damaged hydroxamate, was required for an adequate (but non-unique) fit in addition to components at ~400.8, ~401.4 and ~402.9 eV that could be assigned to N in chemisorbed hydroxamate, N in adsorbed Fe hydroxamate in good electrical contact with the chemisorbed hydroxamate, and N in charge-shifted multilayer Fe hydroxamate in poor electrical contact with the substrate.

The N 1*s* assignments were supported by the spectra determined while the specimen was under the influence of a low energy electron beam. The N 1*s* spectrum then comprised 3 components, one shifted by the full (~4 eV) energy of the flood gun electrons, one shifted by an intermediate energy (~2 eV), and one that was unaffected. These three components would have corresponded, respectively, to N atoms in the multilayer Fe hydroxamate furthest from the substrate, in Fe hydroxamate closer to the substrate, and in hydroxamate chemisorbed to the Fe atoms in the substrate (pyrite surface or Fe oxide at the mineral surface). The component shifted by the full energy was about 50% more intense than the component shifted by the intermediate energy, suggesting that the multilayer on top of the chemisorbed layer would have consisted of 2 to 3 molecular layers of Fe hydroxamate. The substrate Fe 2*p* peaks were unaffected by the electron beam, and not all of the Fe^{III} intensity was shifted the full 4 eV to lower binding energy. The S 2*p* spectrum remained essentially unaffected by the electron beam, which is consistent with all S atoms remaining in the substrate.

The XPS data indicate that during pyrite conditioning in hydroxamate solution, Fe does not migrate from a largely unoxidised mineral surface to form multilayer Fe^{III} hydroxamate, but that Fe is available from an existing oxidised surface layer. That oxidised surface layer would probably consist of Fe hydroxy-oxide rather than Fe_2O_3, and it might provide Fe more readily than the oxide.

Chalcopyrite

Freshly abraded chalcopyrite surfaces exposed to the atmosphere initially oxidise to form hydrated ferric oxide (Buckley and Woods, 1984):

$$CuFeS_2 + 0.75xO_2 + 0.5xH_2O \rightarrow CuFe_{1-x}S_2 + xFeOOH$$

On further exposure to air or alkaline solution, an increasingly intense component from surface Fe^{III}/O species becomes dominant in the Fe 2*p* and 3*p* spectra, an unresolved high binding energy component in the S 2*p* spectrum arises from the Fe-depleted sulfide lattice, and the Cu 2*p* and 3*p* spectra remain essentially unchanged. Thus there would be Fe^{III}/O rather than Cu^{II}/O species at the mineral surface at the onset of conditioning in hydroxamate solution. Freshly abraded chalcopyrite surfaces that had been rinsed with water after being conditioned in hydroxamate solution for periods as short as 1 min were clearly hydrophobic.

For abraded surfaces conditioned in hydroxamate solution for no more than a few minutes, the N 1*s* spectrum (Fig. 7b) was asymmetric but without resolved structure. The spectrum could be fitted with a principal component at ~401.2 eV, a less intense component at ~399.9 eV, and possibly a third component at ~400.8 eV. The highest binding energy component could be assigned to protonated N in ferric hydroxamate and/or co-adsorbed hydroxamic acid, and that near 400.8 eV to hydroxamate chemisorbed to Fe atoms in ferric oxide on the mineral surface. The lowest binding energy component would be consistent with hydroxamate chemisorbed to Cu atoms in the chalcopyrite surface and/or Cu hydroxamate. However, there was no noticeable difference in the Cu 2*p* spectrum before and after conditioning for 1 min, indicating that minimal Cu hydroxamate was formed within that time period. An oxide component near 530 eV in the O 1*s* spectrum remained evident.

After freshly abraded surfaces were conditioning for 10 min, the presence of a Cu^{II} species at the surface was revealed in the Cu 2*p* spectrum, but its concentration was minor compared with that of the Fe^{III}/O species that probably included ferric hydroxamate. Therefore the surface concentration of Cu hydroxamate remained minor, consistent with only very small changes in the less surface sensitive Cu LMM and Cu 3*p* spectra. The corresponding N 1*s* spectrum remained devoid of resolved structure, but for an adequate fit, required a minor component at ~402.7 eV in addition to the three components required in the N 1*s* spectra for brief conditioning periods. This additional component could be rationalised by charge-shifting of co-adsorbed hydroxamic acid and possibly some multilayer ferric hydroxamate, an interpretation supported by the effect of low energy electrons on the individual spectra. Under the influence of the electron beam, the C 1*s*, O 1*s* and N 1*s* spectra all contained components shifted to low binding energy by the full 4 eV electron energy as well as components that were unaffected (Fig. 7c). The Cu 2*p* and S 2*p* spectra remained essentially unchanged, while only minor shifting of the Fe^{III}/O component in the Fe 2*p* spectrum was observed.

The Fe^{III}/O component (from Fe^{III} hydroxamate and oxide) was more intense than for an air-exposed but unconditioned mineral surface, and became increasingly intense with conditioning time. After 10 min conditioning, Fe in the sulfide lattice remained within the depth analysed, nevertheless, the Fe^{III}/O component was more intense relative to the substrate Fe/S component in the Fe 2*p* spectrum than the less surface-sensitive Fe 3*p* spectrum and this would preclude the Fe^{III}/O species being in thick, but not moderately thin, patches. It is most likely that hydroxamate coverage was in patches, adsorbed to initially formed patches of Fe^{III} oxide, given that some Cu^{II}

appears to be formed after longer conditioning. The other spectral features confirming that the coverage of Fe hydroxamate adsorbed at a surface conditioned for 10 min is not large are a moderately low (~6%) surface atomic concentration of N, a Cu 3*p*:Fe 3*p*:S 2*p* intensity ratio that had not changed markedly, and a component near 400.0 eV remaining at least 25% of the total N 1*s* intensity. Loss of Fe hydroxamate from the surface during rinsing could not have been significant, as the metal-deficient sulfide component in the S 2*p* spectrum remained small.

Bornite

Photoelectron spectra for abraded surfaces of bornite conditioned in hydroxamate solution have been reported previously (Parker et al., 2011). More recent XPS data have largely confirmed the earlier findings, however, in rationalising the predominant formation of Cu hydroxamate at pre-oxidised bornite surfaces, there has been more evidence supporting the adsorption of hydroxamate on *patches* of Fe^{III} oxide than for loss of oxide to the aqueous phase. Nevertheless, it remains possible that some of the Fe oxide is removed from the surface in the pH ~9.5 hydroxamate solution. Freshly exposed bornite surfaces oxidise more rapidly than chalcopyrite, and notwithstanding the significantly lower Fe content of bornite, as for chalcopyrite it is the Fe that reacts first to form an oxide or hydroxy-oxide (Buckley et al., 1984; Buckley and Woods, 1983). Under multilayer adsorption conditions, it is usually Cu rather than Fe hydroxamate that has the higher surface concentration, even for pre-oxidised surfaces. This behaviour can be rationalised by the formation of the Fe oxide in patches, and during conditioning, the adsorption of hydroxamate to these Fe oxide patches as well as to Cu in the mineral surface between the oxide patches, and the reaction of hydroxamate with Cu that had migrated through the sulfide lattice to the mineral surface. In other words, Fe oxide formed at the surface prior to conditioning does not markedly hinder the interaction of hydroxamate with Cu. All bornite surfaces treated with hydroxamate in this investigation became hydrophobic.

For minimally oxidised bornite surfaces conditioned for short periods (~1 min), the Cu 2*p* spectrum showed that only a low concentration of Cu hydroxamate could have been present, whereas an Fe^{III}/O component dominated the Fe 2*p* spectrum. However, the overall Cu concentration at the surface was at least a factor of three greater than the overall Fe concentration. It was obvious even without fitting the corresponding N 1*s* spectrum (Fig. 7d) that a ~401.5 eV component arising from protonated hydroxamate N was more intense than a component just below 400 eV attributable to deprotonated N atoms in hydroxamate interacting with Cu in Cu hydroxamate. A better fit to the

spectrum could be obtained by the inclusion of a third component near 400.7 eV that could be assigned to protonated N in hydroxamate chemisorbed to Fe.

Spectra determined while the specimen was bathed in ~4 eV electrons showed some components remained essentially unaffected, some had been shifted to lower binding energy by 1–2 eV, and some had been shifted by the full ~4 eV depending on whether the species from which the peaks arose were in good, partial or poor electrical contact with the bornite substrate. In particular, most of the ~400.0 eV N 1*s* component appeared to have been unaffected, confirming that Cu hydroxamate and hydroxamate chemisorbed to Cu atoms in the bornite surface would have been in good electrical contact with the bornite. Most of the ~401.5 eV N 1*s* component appeared to have been shifted to some extent, including a significant proportion by the full 4 eV, suggesting that the ferric hydroxamate and any co-adsorbed hydroxamic acid was not in good electrical contact with the bornite surface. This is consistent with the oxide component in the O 1*s* spectrum being shifted by more than 2 eV, as that oxide would have been essentially all Fe oxide, and it is expected that the Fe hydroxamate would have been adsorbed to the monolayer of hydroxamate chemisorbed to Fe atoms in the Fe oxide. Furthermore, the Fe oxide would most probably have been in patches rather than a uniform layer.

For 5 min conditioning immediately after abrasion in air, the overall Cu concentration at the surface was lower, but still several times that of Fe, and a slightly greater proportion of the Cu was present as Cu^{II}. There was an obvious oxide component in the O 1*s* spectrum, which correlated with the higher Fe concentration, most of it Fe^{III}/O species, within the depth analysed. The N 1*s* component near 400.0 eV was now marginally more intense than that at ~401.4 eV, which was consistent with the increased Cu^{II} concentration at the surface. An XPS image determined with a resolution of better than 3 μm established that Cu^{II} and N were uniformly distributed on the surface, at least at the μm level.

Thus, under minimal prior oxidation and low collector coverage conditions, there is initially a greater concentration of hydroxamate present as Fe hydroxamate or co-adsorbed hydroxamic acid at a bornite surface than as Cu hydroxamate and hydroxamate chemisorbed to Cu atoms. With increasing conditioning time, Cu hydroxamate becomes increasingly represented at the surface, and can become the major adsorbed species, but the concentration of Fe hydroxamate remains significant.

Conclusions

The interaction of sulfide mineral surfaces with n-octanohydroxamate solutions (pH 9.2 – 9.5) was investigated. Apart from covellite and fractured pyrite surfaces, multilayers of metal hydroxamate were formed on the sulfide minerals investigated. These surfaces were observed to be hydrophobic. Patches of copper and iron hydroxamates were formed on the ternary sulfide minerals. Pyrite did not react significantly with n-octanohydroxamate unless the surface was pre-oxidised. It is, therefore, feasible that flotation of tarnished ores could be achieved with hydroxamate. However, consumption of hydroxamate by non-target minerals (such as pyrite) would need to be depressed.

Acknowledgements

The Australian Research Council, Ausmelt Pty Ltd and Axis House Ltd have provided support for this research project. Dr Ratan Chowdhury has assisted with preparation of purified n-octanohydroxamate compounds and his contribution to the project is gratefully acknowledged.

References

Abraitis, P.K., Brandon, N.P., England, K.E.R., Kelsall, G.H., Lennie, A.R., Pattrick, R.A.D., Vaughan, D.J., Yin, Q., 2000. Electrochemical oxidation of pyrite in alkaline electrolytes: an investigation employing cyclic voltammetry, in situ scanning probe microscopy and ex situ X-ray photoelectron spectroscopy, In *Proceedings of Electrochemistry in Mineral and Metal Processing V, Electrochemical Society*. The Electrochemical Society, pp. 206-216.

Ackerman, P.K., Harris, G.H., Klimpel, R.R., Aplan, F.F., Use of chelating agents as collectors in the flotation of copper sulfides and pyrite. Miner. Metall. Process, 1999, **16**, 27-35.

Buckley, A.N., 2010. Surface chemical characterisation for identifying and solving problems within base metal sulfide flotation plants, In *Flotation Plant Optimisation: A Metallurgical Guide to Identifying and Solving Problems in Flotation Plants*, ed. Greet, C.J. AusIMM, Melbourne, pp. 137-153.

Buckley, A.N., Hamilton, I.C., Woods, R., Investigation of the surface oxidation of bornite by linear potential sweep voltammetry and X-ray photoelectron spectroscopy. J. Appl. Electrochem., 1984, **14**, 63-74.

Buckley, A.N., Woods, R., An X ray photoelectron spectroscopic investigation of the tarnishing of bornite. Aust. J. Chem., 1983, **36**, 1793-1804.

Buckley, A.N., Woods, R., An X-ray photoelectron spectroscopic study of the oxidation of chalcopyrite. Aust. J. Chem., 1984, **37**, 2403-2413.

Buckley, A.N., Woods, R., The surface oxidation of pyrite. Appl. Surf. Sci., 1987, **27**, 437-452.

Das, K.K., Pradip, 1987. Flotation of oxidized chalcopyrite with hydroxamate collectors, In *International Symposium on Interfacial Phenomena in Biotechnology and Materials Processing*, eds. Attia, Y.A., Moudgil, B.M., Chander, S. Elsevier, pp. 305-316.

Evans Jr., H.T., Copper coordination in low chalcocite and djurleite and other copper-rich sulfides. Am. Mineral., 1981, **66**, 807-818.

Fuerstenau, D.W., Herrera-Urbino, R., McGlashan, D.W., Studies on the applicability of chelating agents as universal collectors for copper minerals. Int. J. Miner. Process., 2000, **58**, 15-33.

Fuerstenau, M.C., Miller, J.D., Gutierrez, G., Selective flotation of iron oxide. Transactions of the American Institute of Mining, Metallurgical, and Petroleum Engineers, 1967, **238**, 200-203.

Gardner, J.R., Woods, R., An electrochemical investigation of the natural flotability of chalcopyrite. Int. J. Miner. Process., 1979, **6**, 1-16.

Hanson, J.S., Fuerstenau, D.W., An electrochemical investigation of the adsorption of octyl hydroxamate on chalcocite. Colloids and Surfaces, 1987, **26**, 133-140.

Hanson, J.S., Fuerstenau, D.W., The electrochemical and flotation behaviour of mixed oxide/sulfide ores. Int. J. Miner. Process., 1991, **33**, 33-47.

Hope, G.A., Woods, R., Buckley, A.N., White, J.M., McLean, J., Spectroscopic characterisation of n-octanohydroxamic acid and potassium hydrogen n-octanohydroxamate. Inorg. Chim. Acta, 2010a, **363**, 935-943.

Hope, G.A., Woods, R., Parker, G.K., Buckley, A.N., McLean, J., A vibrational spectroscopy and XPS investigation of the interaction of hydroxamate reagents on copper oxide minerals. Miner. Eng., 2010b, **23**, 952-959.

Hope, G.A., Woods, R., Parker, G.K., Buckley, A.N., McLean, J., Spectroscopic characterization of copper acetohydroxamate and copper n-octanohydroxamate. Inorg. Chim. Acta, 2011, **365**, 65-70.

Hughes, T., Lee, K., Sheldon, G., Bygrave, J., and Mann, L. 2007. In 2007. The application of Ausmelt's AM28 alkyl hydroxamate flotation reagent to Fox Resources' West Whundo copper ore at Radio Hill, Western Australia, In *Proc. Ninth Mill Operators' Conference*. AusIMM, Fremantle, Western Australia, 19-21 March, 2007, pp. 51-54.

Lee, K., Archibald, D., McLean, J., Reuter, M.A., Flotation of mixed copper oxide and sulfide minerals with xanthate and hydroxamate collectors. Miner. Eng., 2009, **22**, 395-401.

Lehmann, M.N., Stichnoth, M., Walton, D., Bailey, S.I., The effect of chloride ions on the ambient electrochemistry of pyrite oxidation in acid media. J. Electrochem. Soc., 2000, **147**, 3263-3271.

Parker, G.K., Hope, G.A., Woods, R., Numprasanthai, A., Buckley, A.N., McLean, J., 2011. Investigation of the n Octanohydroxamate Reagent Interaction with the Surface of Oxide Copper Minerals and Copper Metal, In *Yoon Symposium, 2011 SME Annual Meeting*, ed. Young, C. SME, Denver, Colorado, p. Accepted 02/2011.

Parker, G.K., Woods, R., Hope, G.A., 2003. Raman investigation of sulfide leaching, In *Hydrometallurgy 2003 - Fifth International Conference in Honor of Professor Ian Ritchie*, eds. Young, C.A., Alfantazi, A.M., Anderson, C.G., Dreisinger, D.B., Harris, B., James, A. TMS, Vancouver, Canada, pp. 447-460.

Pöpperle, J., *Froth flotation of ores*. 1940, Fried. Krupp Grusonwerk Akt.-Ges., DE 700735.

Schaufuß, A.G., Nesbitt, H.W., Kartio, I., Laajalehto, K., Bancroft, G.M., Szargan, R., Incipient oxidation of fractured pyrite surfaces in air. J. Electron Spectrosc. Relat. Phenom., 1998, **96**, 69-82.